Establishment and setting up of the lab equipment

Deliverable D_3.2.1

Contributing partners:

LP – UNIPD DICEA

Section 1

Theoretical and numerical analysis of the laboratory model setup

TABLE OF CONTENTS

1. Introduction

Subsurface formations are known to display spatial variability of the properties (Dagan and Zeitoun 1998, Freeze (1975)). However, the assumption of homogeneity is normally applied, though a simplification respect to reality. This report focuses on the effect of heterogeneity of the porous media and considers different random realizations of heterogeneity field of hydraulic conductivity, K. The method is aimed at defining the influence of heterogeneity fields in order to reproduce "real" laboratory fields to be applied for laboratory activities. From the practical point of view, this approach is preliminary to the definition of the beads size to be used in the laboratory accordingly to market availability. For this purpose, a large number of 2D anisotropic heterogeneous random sand structures (with given mean, variance and horizontal and vertical correlation length) were generated. Some of them were used as porous media in saltwater intrusion numerical simulations using the Finite Elements code SUTRA and provides basic information and results for future studies and developments which include laboratory modeling of saltwater intrusion in heterogeneous formations.

2. Physical model setup by modelling

1.1 Preliminary random field generation

The process starts with the generation of a sequence of random numbers of hydraulic conductivity using a log – normal distribution: each of the generated number will represent a value of hydraulic conductivity in the heterogeneous field (see figure 1, panel a)). The domain corresponds to the dimension of the physical model to be used containing 250 values. The physical model is a hydraulic channel 5 m long, 0.5 m height, and 0.3 m wide (Figure 1, panel b)). The axis origin of the domain, the (0, 0) coordinates point corresponds to the upper point of the inland boundary. The domain is subdivided into three parts: a left-hand side, a central, and a right-hand side. The left-hand side is the one with the larger mesh, having an element size of 2.5 · 10−3 m x 2 · 10−2 m. In this part of the domain gradient of concentration is not present during the simulation and the dominant flow direction is always horizontal. The right-hand side has the finer mesh with elements of 2.5 · 10−3 m x 5 · 10−3 m, because in this part salt transport and changes in flow direction occur and a more accurate solution is needed. The central part has element size of 2.5·10−3 m x 10−2 m and has the role of making the transition between the left-hand side and the

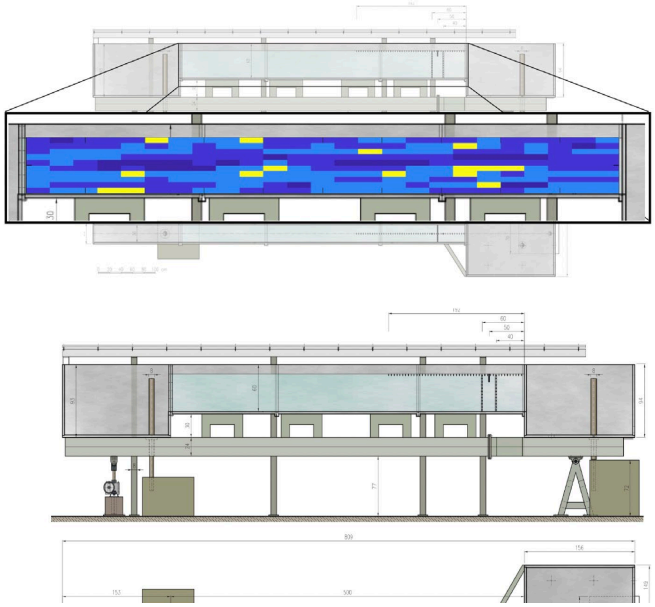

Figure 1:conductivity random fileds (panel a)) and laboratory setting (panel b))

right-hand side smoother. This spatial discretization represented a good compromised between solution accuracy and computational effort.

1.2 Numerical settings

A hydraulic gradient between upstream and downstream side is necessary to have flow from inland toward the sea. In this case the hydraulic gradient is 2 cm. A different pressure distribution is still needed for the change in velocity field to occur: at inland boundary, a hydrostatic pressure distribution is imposed according to base concentration density, that is at zero concentration, using ρ0 = 1000 kg/m3, whereas, at seaside boundary the pressure distribution is still hydrostatic but calculated with maximum concentration density. This condition determines the flow and allows the intrusion of salt through the seaside boundary as function of the velocity field. This boundary conditions are maintained during the whole simulation time and for all simulations, only the hydraulic conductivity distributions changes. The soil matrix is considered to be isotropic and the relation used to model the water content in unsaturated condition as function of the pressure head is the Van Genuchten (1980) and the Mualem (1976) one. Longitudinal and transversal dispersivities are crucial parameters that deeply affect the final concentration distribution, in particular the length of the wedge toe and the thickness of the transition zone; the two dispersivity values depend on the mesh size (scale effect).

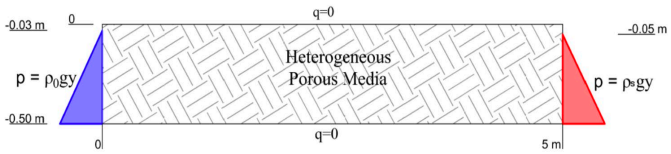

Figure 2: simulation model

1.3 Recharge simulations

Artificial groundwater recharge is a technique used to mitigate saltwater intrusion by locally rising the piezometric surface, creating higher hydraulic gradient, contrasting the salt wedge advancement. The recharge can be natural, by infiltration and percolation of precipitation and run-off, artificial, spreading water on the surface or injected it with wells, or induced, that consists in a modification of the freshwater level upstream as consequence of an external factor such as check dams or flood control systems. Artificial recharge consists of the injection of freshwater by means of infiltration wells or infiltration channels. This solution creates a sort of barrier by locally increasing hydraulic head, allowing to control seawater intrusion inland. Infiltration wells are generally placed along a parallel line to the coast. Numerical simulations aimed at modelling this process were carried out, imposing a specific freshwater flow from the upper boundary. The recharge is assumed to be Qr=0.5kg/h. This freshwater flow is set to be uniformly distributed along a linear surface of 0.5 m. Three different recharging areas are selected: the first one is centered at x = 3.5, the second is centered at x = 4m, and the third is centered in x = 4.5 m to enquire the best location for the injection point.

3. Results

1.4 Clustering results and fields selection

Practically speaking, different values of hydraulic conductivity correspond to different value of particle-size of the soil matrix given the equation proposed by Kozeny (1927). However, to make the randomly generated field of hydraulic conductivity physically reproducible (i.e. to perform laboratory experiments in future), a clustering process was performed, and four different classes of beads size were defined corresponding to a specific value of hydraulic conductivity, K (see table 1).

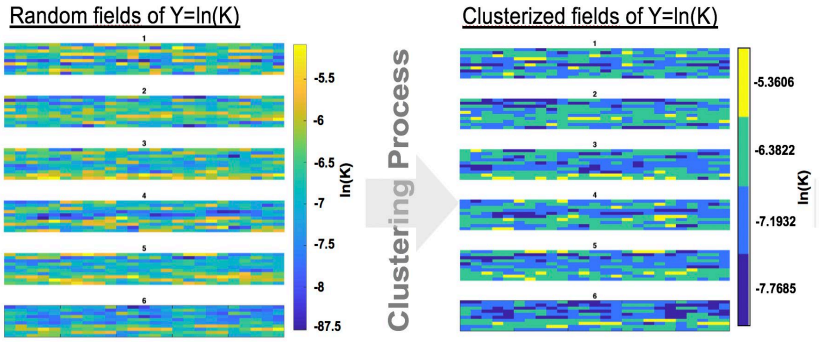

Figure 3:random clustering proceudure

The clustering approach allowed to move from the original randomly generated fields to "real" experimental fields, as illustrated in figure 3 (where the data are presented in the log-normal domain and back-transformed after the clustering analyses): it allows to make the random fields physically reproducible, linking the hydraulic conductivities to a diameter class available in the market. Starting from these results, a selection of 10 scenarios was made to perform the numerical simulation due to computational time reasons.

Table 1: clustering procedure (Kozeny (1927))

Beads size	[µm]		Hydraulic conductivity	[m/s]
d_1	300 – 400	→	K_1	4.228E-4
d_2	400 – 600	→	K_2	7.517E-4
d_3	600 – 800	→	K_3	1.693E-3
d_4	1000 - 1200	→	K_4	4.698E-3

1.5 Numerical simulations

In figure 4 the concentration isoline equal to 50 % was reported for the whole ensemble at different injection points both in case of recharge (blue lines, averaged over the ensemble) and in case of free injection (i.e. without the recharge, red lines, averaged over the ensemble) at different times. A vertical displacement is defined, calculated as the difference, at a given horizontal position, between the quote of the free intrusion and the solution with freshwater recharge. The recharging process starts at t= 24 hours. At the beginning of the recharging process, the forces induced by water flow from the upper part of the domain, in some cases (i.e. some hydraulic conductivity distribution), can cause the rising of the interface, which is here displayed as a negative displacement. Figure 5, in each panel, reports the vertical displacement in time for the three different location of the injection points. The green, red and blue curves are averaged over the entire ensemble for the different injection points.

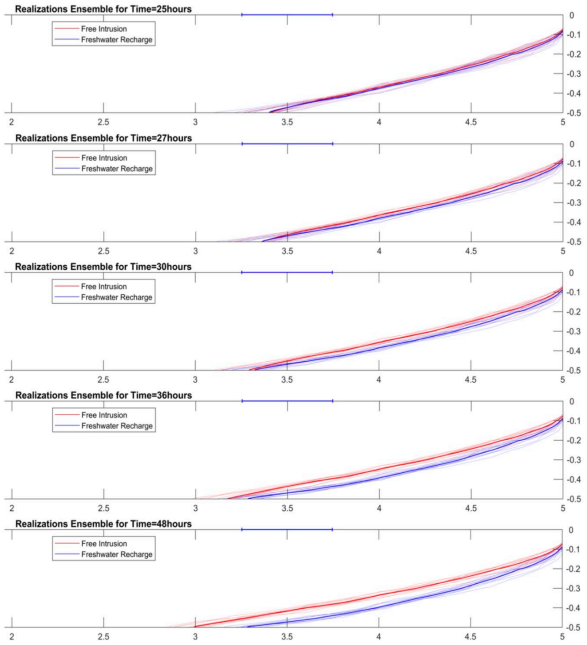

Figure 4: Artificial recharge simulations

At the beginning of the recharging process, the forces induced by the water flow from the upper part of the domain, in some cases (i.e. some hydraulic conductivity distribution), can cause a rising of the interface, which is here displayed as a negative displacement. The green curve (recharge at x = 3.5 m) has the higher time derivative, and this means that, given the same time interval, it is the one that increases the most, providing the greatest lowering effect on the interface. The time series of the toe length for the three recharge conditions and for free are reported in figure 6. It can be appreciated that the recharge has the effect of decreasing the velocity of advancement of the intruding wedge and just in the case of recharge at x = 3.5m this velocity becomes negative. This means that, to retreat the intrusion process, the more upstream the recharge is placed, the better effect on the toe length is obtained. Of course, it is necessary to ensure that the infiltrated or injected freshwater reaches the intruding wedge and does not disperse laterally. This behavior can be explained through a balance of the forces involved: if the recharge is placed over the intruding wedge it can cause a significant local lowering of the interface, but just a part of it contributes to the horizontal force balance with the intruding wedge, while a fraction of the recharge flushes out by the flow pattern through the freshwater outlet. If the recharge is made more upstream than the intruding wedge, the whole recharge amount takes part in contrasting the advancement of saltwater intrusion.

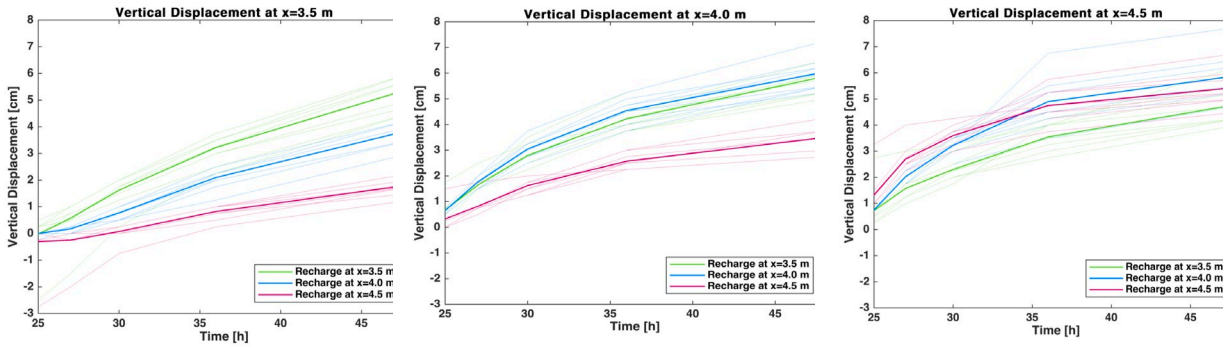

Figure 5: time evolution of the vertical displacement for three different inject locations

4. Conclusions of modelling setup

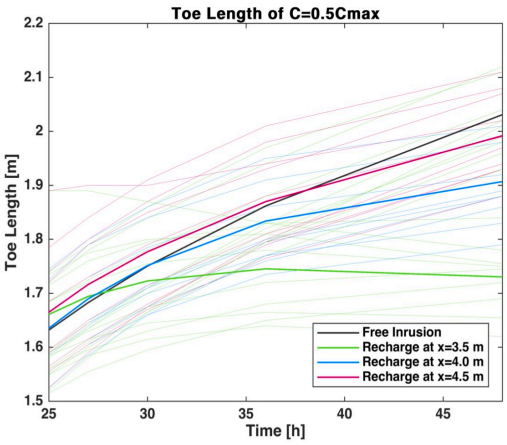

Figure 6: toe length influence

The generation of heterogeneous fields reproducible in the hydraulic laboratory of the department of civil, environmental and architectural engineering was analyzed at first. A generation process is carried out in order to reproduce a large number of synthetic sand structures, starting with a normally distributed random number generator. For these reasons, a clustering process, based on the Kozeny (1927) relation was applied to define the beads size between the ones available in the market available. The generated hydraulic conductivity values were clusterized in four classes. Free intrusion phenomenon is then analyzed, using as input of the numerical model the same domain geometry and boundary conditions applied in the experimental activities with changing permeability distribution. Results were analyzed in terms of concentration distribution. The heterogeneity in hydraulic conductivity influences the flow of groundwater, modifying the velocity distribution and creating preferential pathways for the flow, affecting the geometry of the interface between freshwater and saltwater, as well as the location of the freshwater discharge on the seaside boundary. Then, freshwater artificial recharge by means of infiltration wells or channel is numerically tested: once the intrusion process is well developed, artificial groundwater recharge processes were simulated. The only case, between the analyzed ones, in which this velocity becomes negative, meaning that the salt wedge is retreating, is when the recharge is located upstream than the intruding wedge. From these evidences, it can be concluded that, unless a locally control and lowering of the interface is needed, the location of the recharge area upstream to the interface zone gives better results in terms

of retreating of the salt wedge and general vertical displacements of the freshwater-saltwater interface. In conclusions it is possible to say that this work represents a starting point for future further studies on the process of saltwater intrusion in heterogeneous formations, both numerical and experimental.

5. Hydraulic conductivity evaluation

The aim of the research is to experimentally estimate and tested the hydraulic conductivity (K, [m/s]) for the four different classes (i.e. four different samples) identified from the numerical simulation analysis of report 3.2.1,

Beads size class	[µm]
d_1	300 – 400
d_2	400 – 600
d_3	600 – 800
d_4	1000 - 1200

6. Data and Methods

A single sample was collected for each of the four classes. Permeameter laboratory investigations have been performed on each sample in four different days, while granulometry analysis in three. In each day:

Permeability tests	**Granulometry analysis**
23 October 2019	24 October 2019
30 October 2019	-
5 November 2019	5 November 2019
14 November 2019	14 November 2019

The analysis starts testing the four different classes; then, accordingly to the results obtained from the permeability tests and the granulometric analysis on 23 October 2019; then, the analysis focuses on the second and the third classes for the other three days. Permeability test consists of three different experiments on the same sample: this mean that the final value of hydraulic conductivity, K, is averaged over a group of three.

A permeameter is applied with the following characteristics:

d	7.38	cm
A	42.776	cm^2

In the following the samples used for the conductivity tests and the granulometry analysis ar e reported. The dimensions of the sieves used for the granulometric analysis are reported in the following:

Number of the sieve	**d sieve [mm]**
3"	76.2
2"	50.8
1"1/2	38.1
1"	25.4
3/4"	19.1
1/2"	12.7
3/8"	9.52
4	4.76
10	2
20	0.84
40	0.42
60	0.25

80	0.177
140	0.105
200	0.074

In the following, tables with data regarding the physical characteristics of the samples applied to perform the permeability tests and granulometric analysis are reported according to the day and the class.

23 October 2019

Permeability Sample data

	I sample	II sample	III sample	IV sample
D [µm]	300 - 400	400 - 600	600 - 800	1000 - 1300
P sacc [g]	4104	4721	4067	4189
P1 [g]	2662.3	2662.3	2662.3	2662.3
P netto [g]	1441.7	2058.7	1404.7	1526.7
H [cm]	24	23	22	22.8

Sieve analysis samples

	I sample	II sample	III sample	IV sample
d [µm]	300 - 400	400 - 600	600 - 800	1000 - 1300
Pnetto [g]	105.9	101.5	100.6	107.5

30 October 2019

Permeability Sample data

	I sample	II sample	III sample	IV sample
D [µm]	300 - 400	400 - 600	600 - 800	1000 - 1300
P sacc [g]		4002	3956.6	
P1 [g]		2654.2	2654.2	
P netto [g]		1347.8	1302.4	
H [cm]		23	22	

5 November 2019

Permeability Sample data

	I sample	II sample	III sample	IV sample
D [µm]	300 - 400	400 - 600	600 - 800	1000 - 1300
P sacc [g]		4853	4848	
P1 [g]		3305.6	3305.6	
P netto [g]		1547.4	1542.4	
H [cm]		23.5	24.5	

Sieve analysis samples

	I sample	II sample	III sample	IV sample
d [µm]	300 - 400	400 - 600	600 - 800	1000 - 1300
Pnetto [g]	-	265	270.7	-

14 November 2019

Permeability Sample data

	I sample	II sample	III sample	IV sample
D [µm]	300 - 400	400 - 600	600 - 800	1000 - 1300
P sacc [g]		4853	4006	
P1 [g]		2659.6	2659.6	
P netto [g]		2193.4	1346.4	
H [cm]		23.5	24.5	

Sieve analysis samples

	I sample	II sample	III sample	IV sample
d [µm]	300 - 400	400 - 600	600 - 800	1000 - 1300
Pnetto [g]		307	327.5	

7. Results

In the following, the results of the permeability tests and granulometric analysis are reported, day by day and sample by sample.

Permeability tests and granulometric analysis have been performed on the four samples on October 23, 2019; then, the analyses focus on the II and III samples which have been reported similar values of permeability (this is the reason why tables are reported only for the II and III classes). At each time, for each class three permeability test are performed so that the final value of the hydraulic conductivity is averaged over the three results.

23 October 2019

Permeability tests

		Q [l/s]	K [m/s]	K_m [m/s]
Sample 1	T1	1.92E-03	9.33E-04	**8.85E-04**
	T2	3.19E-03	8.89E-04	
	T3	6.81E-03	8.33E-04	
Sample 2	T1	4.63E-03	3.61E-03	**3.07E-03**
	T2	7.76E-03	3.95E-03	
	T3	9.48E-03	1.67E-03	
Sample 3	T1	3.64E-03	3.70E-03	**3.34E-03**
	T2	1.06E-02	3.54E-03	
	T3	1.17E-02	2.77E-03	
Sample 4	T1	6.20E-03	1.21E-02	

T2	9.26E-03	1.14E-02	**1.11E-02**
T3	1.75E-02	9.96E-03	

Granulometric curves

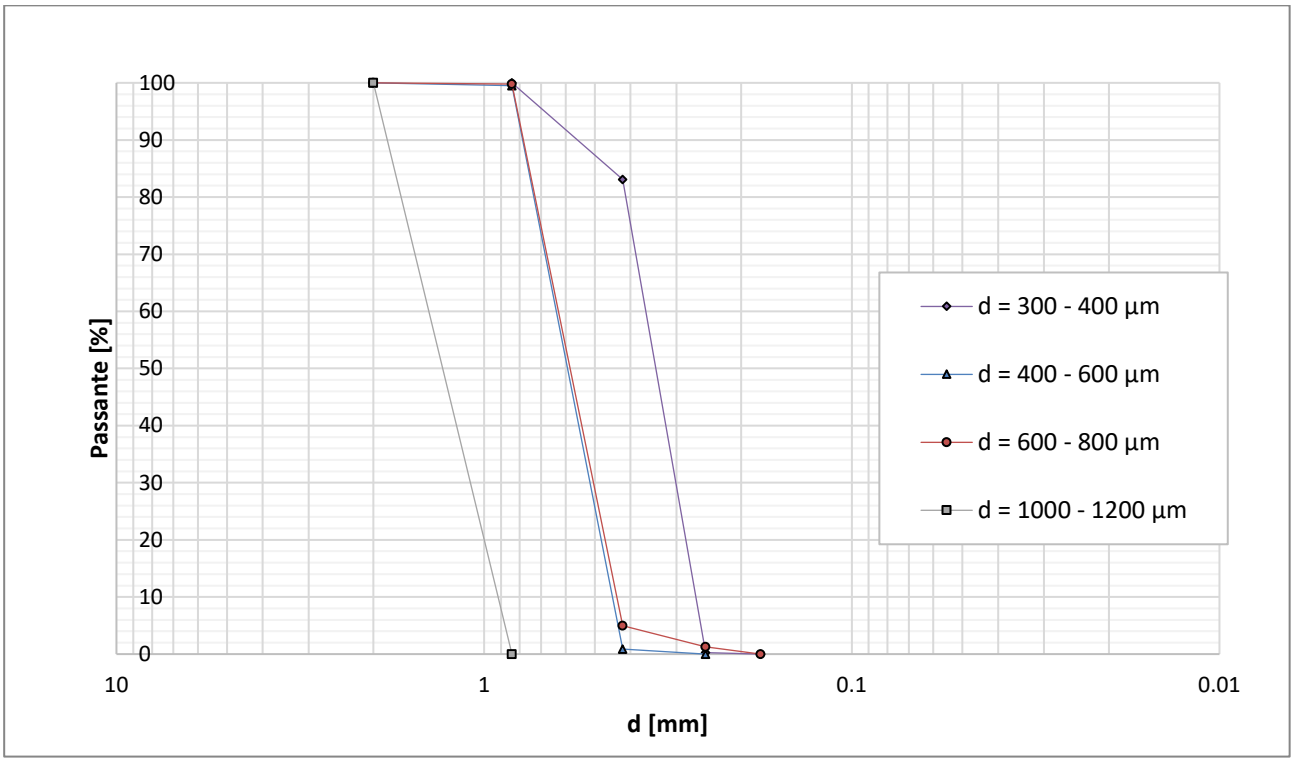

30 October 2019

Permeability tests

		Q [l/s]	K [m/s]	K_m [m/s]
Sample 2	T1	3.68E-03	4.77E-03	4.64E-03
	T2	7.45E-03	4.84E-03	
	T3	1.03E-02	4.31E-03	
Sample 3	T1	3.78E-03	3.16E-03	3.12E-03
	T2	4.99E-03	2.99E-03	
	T3	8.40E-03	3.22E-03	

5 November 2019

Permeability tests

		Q [l/s]	K [m/s]	K_m [m/s]
Sample 2	T1	2.21E-03	3.97E-03	3.91E-03
	T2	3.62E-03	4.03E-03	
	T3	5.44E-03	3.74E-03	
Sample 3	T1	2.71E-03	3.52E-03	3.17E-03
	T2	4.81E-03	3.21E-03	
	T3	6.94E-03	2.80E-03	

Granulometric curves

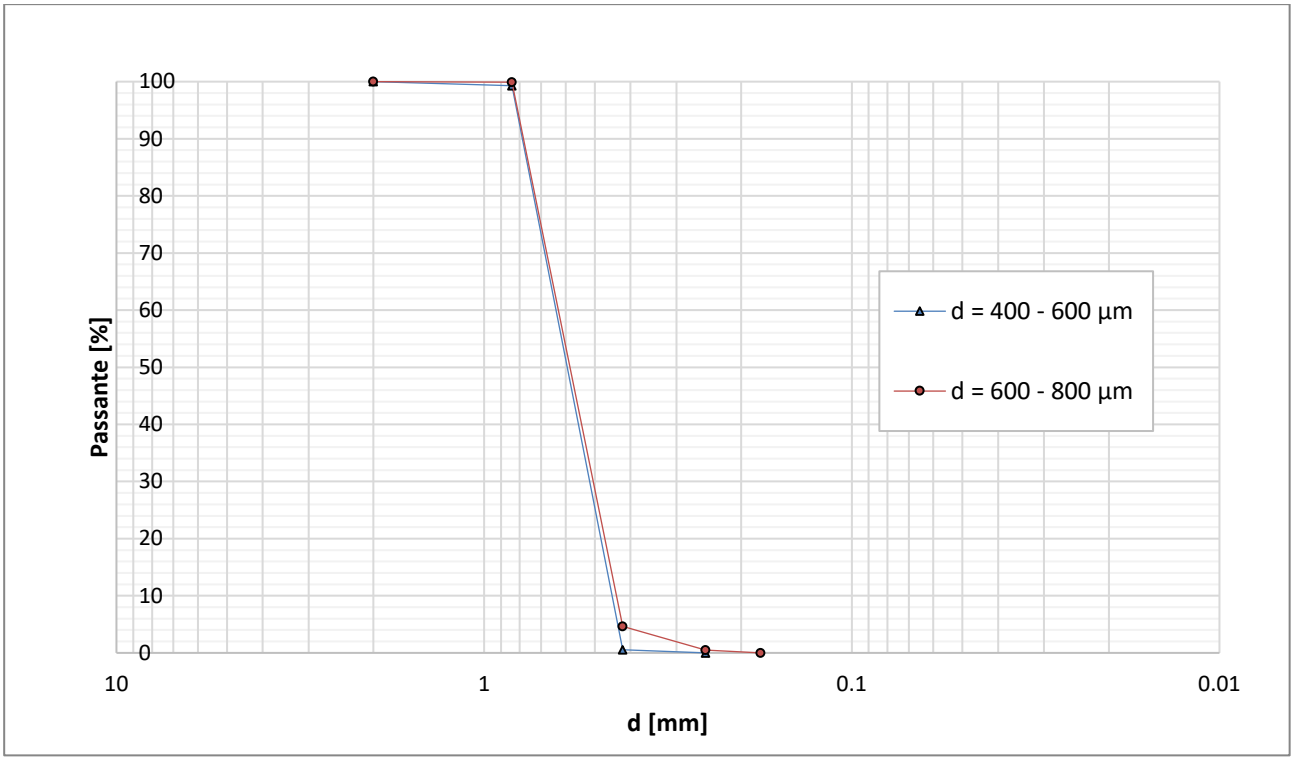

14 November 2019

Permeability tests

		Q [l/s]	K [m/s]	K_m [m/s]
	T1	3.64E-03	3.55E-03	
Sample 2	T2	5.61E-03	3.12E-03	3.24E-03
	T3	8.58E-03	3.04E-03	

	T1	3.43E-03	3.64E-03	
Sample 3	T2	6.36E-03	3.10E-03	3.28E-03
	T3	7.93E-03	3.09E-03	

Granulometric curves

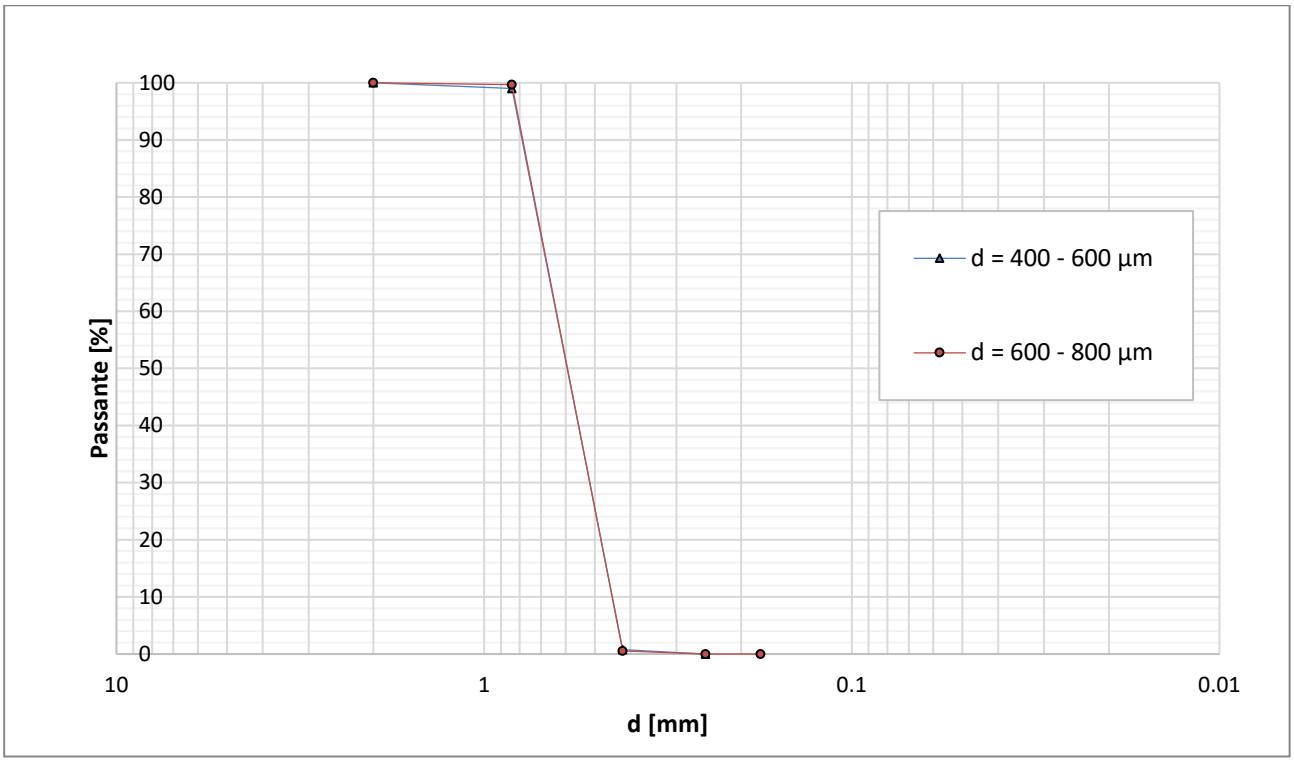

1.1 Hydraulic conductivity estimation: a comparison

Once performed the laboratory tests, these values and the ones obtained through numerical random simulations are compared. It can been appreciated that the laboratory values of conductivity of class II and III are very similar and in general small differences are reported between the estimates.

Beads size	[µm]		[m/s]	Hydraulic conductivity_numerical simulations	Hydraulic conductivity_laboratory tests
d_1	300 – 400	→	K_1	**4.228E-4**	**8.85E-04**
d_2	400 – 600	→	K_2	**7.517E-4**	**3.90E-03**
d_3	600 – 800	→	K_3	**1.693E-3**	**3.23E-03**
d_4	1000 - 1200	→	K_4	**4.698E-3**	**1.11E-02**

8. Conclusions

Previous graphs show that the II and III classes report very similar values of hydraulic conductivity: these experimental evidences from the laboratory tests allow us to group together these two classes and use just three classes for the future analyses. The comparison between the hydraulic conductivity values obtained from the laboratory tests and the ones from the numerical random simulations reports small differences.

9. References

Kozeny, Josef (1927). “Uber grundwasserbewegung”. In: Wasserkraft und Wasserwirtschaft 5.

Dagan, Gedeon and David G. Zeitoun (1998). “Seawater-freshwater interface in a stratified aquifer of random permeability distribution”. In: Journal of Contaminant Hydrology 29.3, pp. 185–203.

Freeze, R A and J. A. Cherry (1979). Groundwater. Englewood Cliffs, New Jersey.

Nicola Cogo, (2019), “Laboratory Setup on Saltwater Intrusion in Heterogeneous Formations through Numerical Experiments”, Master thesis

Section 2

Setting-up of the experimental canal

Setting-up of the experimental canal

Studying and monitoring the dynamic nature of the freshwater-seawater transition zone is of primarily importance not only to guarantee water supply for human activities and to avoid degradation of coastal aquifers, making them unusable, but also to preserve and to protect coastal ecosystems and their biodiversity, sensitive to changes in water salinity concentrations, and the relative introduction of excess nutrients by groundwater.

To this aim in the laboratory od the ICEA Department a set of experiments that aims to reproduce saltwater intrusion phenomena in a controlled heterogeneous media is under development.

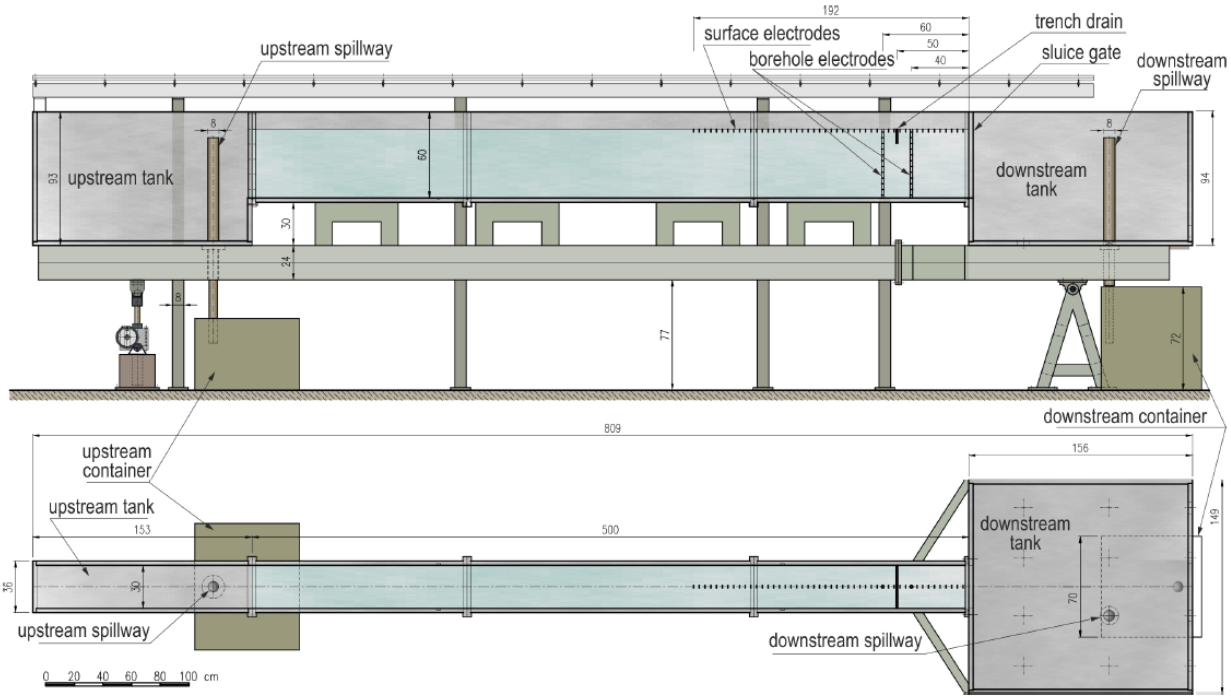

Figure 6 – Longitudinal section and plan of the laboratory canal used to develop experiments on saltwater intrusion

The laboratory canal used in this study is represented in Figure 4: it measures 500 cm long by 30 cm wide by 60 cm high, with 3 cm thick plexiglass walls. Two tanks are located upstream and downstream from the sandbox, with maximum volume capacities of 0.41 m^3 and 1.93 m^3, respectively. The upstream tank is filled with freshwater and is continuously supplied by a small pump, providing freshwater recharge. The downstream tank, filled with salt water, represents the sea. Both tanks are equipped with a spillway that, by discharging the excess flow, guarantees a constant water level, which is also continuously measured by

ultrasonic sensors, allowing us to monitor the gradient and to check that it does not change or fluctuate during the experiment (Crestani et al., 2022).

As reported in previous delivery reports, a huge work was developed in the past to identify by numerical modeling a proper heterogeneous structure representative of a natural but controlled aquifer, i.e. of known physical properties, mainly porosity and hydraulic conductivity spatial distribution, choosing at the end the one represented in Figure 5.

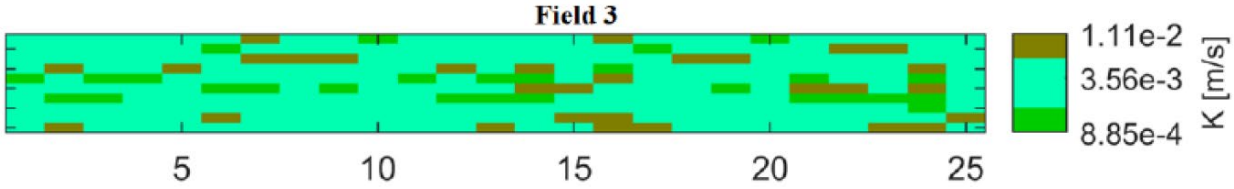

Figure 7 - Heterogeneous aquifer scheme to be reproduced

The porous medium in the sandbox is obtained by means of glass beads characterized by three different nominal size ranges, equal to 0.3-0.4, 0.4-0.8 and 1.0-1.3 mm respectively. The main advantage of using glass beads is the absence of chemical interactions between the dye and salt mixture with the porous matrix, which allows for multiple test repetitions (Crestani et al., 2022).


Figure 8 - Specially manufactured steel blades used to realize volumes at multiple distances of 20 cm in the same 5 cm thick layer

Figure 9 - Glass beads laying activities

The porous medium was packed into the sandbox under dry conditions: the beads were arranged layer by layer, using specially manufactured steel blades (Figure 6) to place different grain size volumes at multiple distances of 20 cm in the same 5 cm thick layer. Each layer was compacted with a 4 kg weight falling from a height of 20 cm on a wooden board as wide as the channel and 2 m long to even out the load. The laying operations (Figure 7) continued until the planned height of 50 cm, the entire thickness of the aquifer, was reached.

The obtained final configuration of the heterogeneous sandbox is shown in Figure 8. The hydraulic conductivity values of each nominal size range have been previously assessed (MoST_LP_3.2.1_set_lab_equipments_periodII and MOST_LP_3.4.5_efficiency_mitigation_strategies _climate_change_periodIII) but the laying activities can certainly alter the values obtained by the permeameter and a global assessment of the hydraulic properties has been developed.

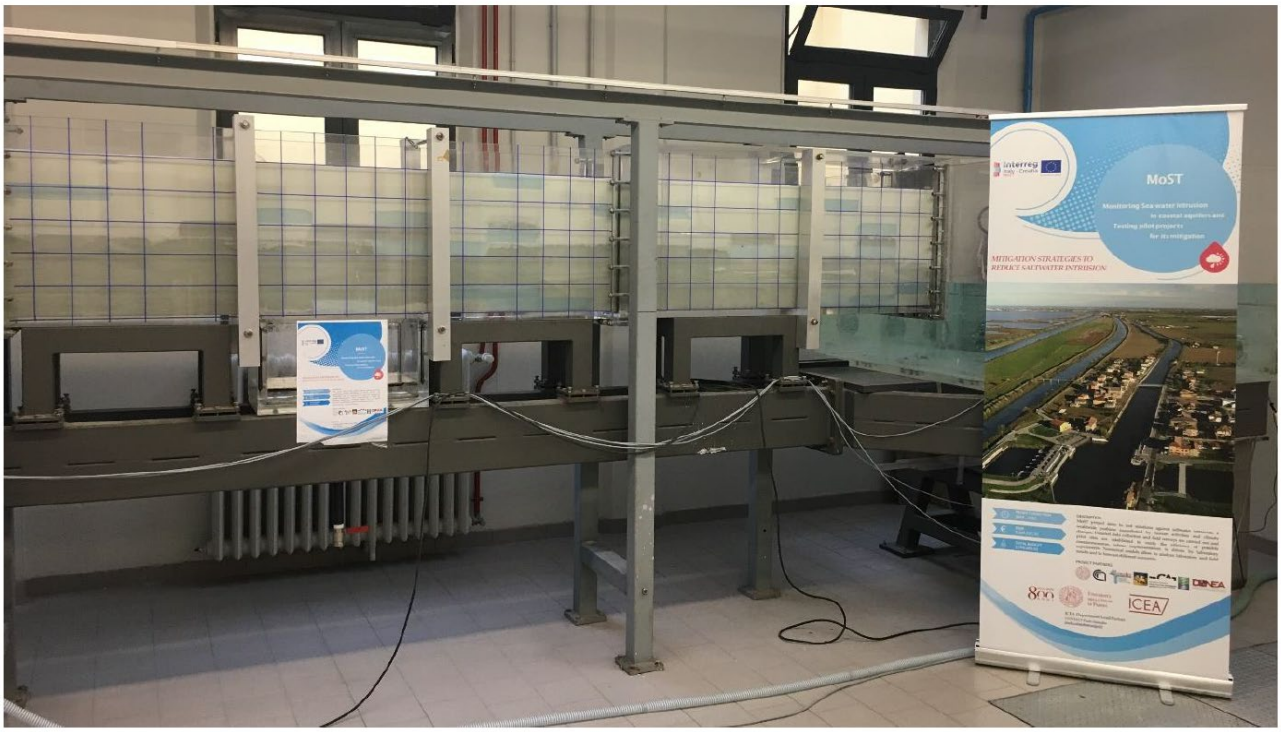

Figure 10 - Final configuration of the heterogeneous sandbox

Preliminarily we proceeded with a slow filling process of the porous mass starting from the bottom and going up by 10 cm steps, maintaining each step for at least 12 hours to ensure the evacuation of air bubbles trapped in the pores.

To achieve the hydraulic conductivity measurements, the experiments considered three different gradients (0.4%, 0.8% and 1.2%) of the water table for each downstream boundary condition, set equal to 10, 20, 30 and 40 cm, for a total of 12 experiments.

To reach a stable configuration the duration of each experiment was almost 12 hours. In Table 1 the long-time results of the experiments analyzed according to the Dupuit relationship are reported. As expected the values are varying according the different downstream boundary condition, i.e. the mean aquifer depth affected by the filtration process.

Table 2 - Values of hydraulic conductivity obtained from experimental results

test no.	upstream depth (cm)	downstream depth (cm)	discharge (l/s)	hydraulic conductivity *1000 (m/s)

1	46	40	0.2285	2.46
2	44	40	0.1587	2.62
3	42	40	0.0792	2.68
4	36	30	0.2329	3.27
5	34	30	0.1549	3.36
6	32	30	0.0662	2.96
7	26	20	0.1682	3.39
8	24	20	0.1162	3.67
9	22	20	0.0564	3.73
10	16	10	0.1214	4.32
11	14	10	0.0823	4.76
12	12	10	0.0419	5.30

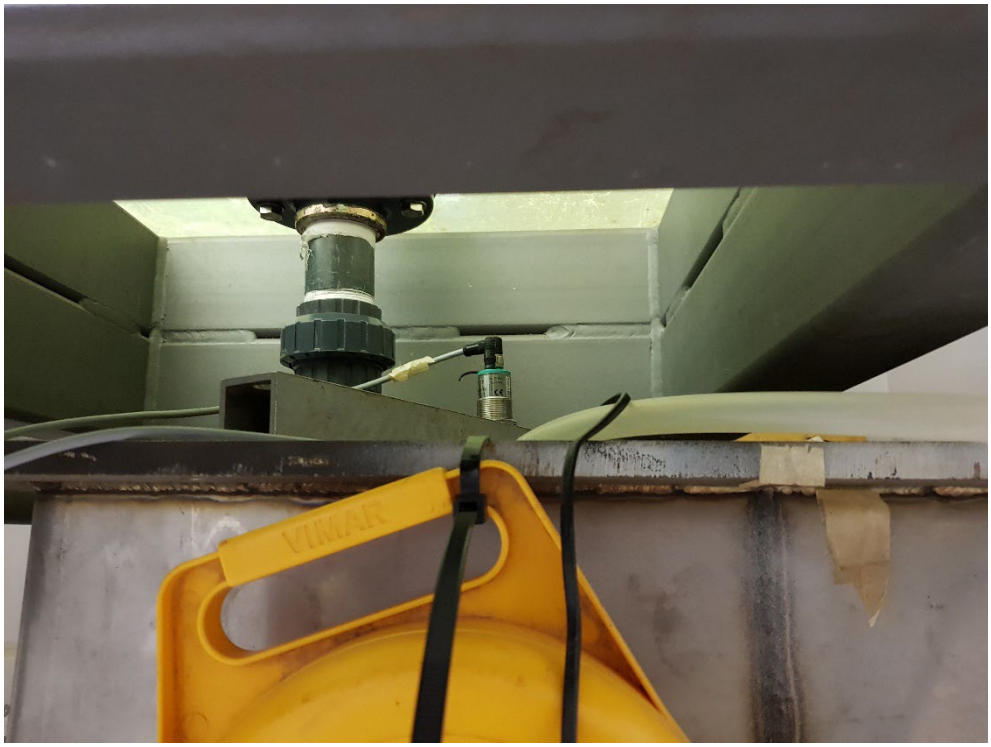

Figure 11 – Sensor system of the downstream metering tank: lateral view

The drain is controlled with a volumetric technique, measuring the water level in a cylinder of known geometry which is filled by the outflow. The cylinder has a limited area to ensure the measurement

accuracy, so it is often necessary to empty it manually. To ensure long-term metering, a pump controlled by a contactor (a particular type of relay used for switching on or off an electrical circuit) has been set up to automatically empty the metering tank when the water reach a prescribed level (Figure 9 and Figure 10).

Figure 12 - Sensor system of the downstream metering tank: downstream view